

Effective Reinforcement Learning Control using Conservative Soft Actor-Critic

Zhiwei Shang^{1†}, Xinyi Yuan^{2†}, Wenjun Huang³, Yunduan Cui³, Di Chen⁴, Meixin Zhu^{5*}

Abstract—Reinforcement Learning (RL) has shown great potential in complex control tasks, particularly when combined with deep neural networks within the Actor-Critic (AC) framework. However, in practical applications, balancing exploration, learning stability, and sample efficiency remains a significant challenge. Traditional methods such as Soft Actor-Critic (SAC) and Proximal Policy Optimization (PPO) address these issues by incorporating entropy or relative entropy regularization, but often face problems of instability and low sample efficiency. In this paper, we propose the Conservative Soft Actor-Critic (CSAC) algorithm, which seamlessly integrates entropy and relative entropy regularization within the AC framework. CSAC improves exploration through entropy regularization while avoiding overly aggressive policy updates with the use of relative entropy regularization. Evaluations on benchmark tasks and real-world robotic simulations demonstrate that CSAC offers significant improvements in stability and efficiency over existing methods. These findings suggest that CSAC provides strong robustness and application potential in control tasks under dynamic environments.

I. INTRODUCTION

Reinforcement Learning (RL) has emerged as a powerful method for learning optimal control strategies in complex and dynamic environments without relying on prior knowledge [1], with broad success in robotic control and game playing [2]–[7]. When deep neural networks [8] are combined with the Actor-Critic (AC) architecture [9], RL can effectively handle high-dimensional state and action spaces, achieving superhuman performance across challenging domains [10]–[15]. However, deploying RL in real-world systems requires careful balancing of sample efficiency, learning stability, and control performance [16]–[18]. To address this, researchers have explored entropy and relative entropy regularization to optimize the exploration-exploitation trade-off.

Soft Actor-Critic (SAC) [19], a representative Maximum Entropy RL method, uses entropy regularization to encourage exploration and has achieved strong results in various control tasks [20]–[23]. However, maximizing policy entropy can destabilize learning, leading to overly aggressive updates when policy-entropy dynamics are misaligned or the

TABLE I: Comparison of CSAC and the related approaches

Approach	Entropy	Relative Entropy
TD3 [30]	×	×
PPO [25]	×	○
SAC [19]	○	×
CSAC (ours)	○	○

environment changes significantly. In contrast, Trust Region Policy Optimization (TRPO) [24] and Proximal Policy Optimization (PPO) [25] use relative entropy constraints to limit update magnitudes, improving stability but often at the cost of sample efficiency in on-policy settings [26]–[29].

Despite these advances, few works have integrated both entropy and relative entropy regularization within an AC framework for continuous control. Prior methods such as Dynamic Policy Programming (DPP) [31] and Conservative Value Iteration (CVI) [32] have demonstrated the benefits of combining these regularization techniques in value-based settings, with extensions further validating their potential [33]–[36]. However, the computational complexity of SoftMax operations in continuous action spaces has largely confined these methods to discrete settings.

To address this gap, we propose Conservative Soft Actor-Critic (CSAC), which integrates entropy and relative entropy regularization within the AC framework. CSAC uses entropy regularization in the critic’s Q-function to promote exploration, while relative entropy regularization constrains policy updates to ensure stability and robustness. As summarized in Table I, the contributions of this paper are:

- 1) We develop an RL method that combines entropy and relative entropy regularization, unifying the stability of PPO with the exploration capability of SAC, and demonstrate significant improvements in sample efficiency and learning stability across various control tasks.
- 2) We extend the principles of CVI and DPP to continuous action spaces within the AC framework without introducing additional computational complexity, broadening the applicability of entropy-constrained RL to complex continuous control tasks.
- 3) Through extensive experiments on benchmark tasks and Real-Robot-Based simulations, we validate that CSAC significantly outperforms existing RL algorithms in learning stability, sample efficiency, and final policy performance.

[†]Zhiwei Shang and Xinyi Yuan have contributed equally to this work.

* Corresponding author: Meixin Zhu (e-mail: meixin@ust.hk)

¹ School of Data Science, The Chinese University of Hong Kong, Shenzhen, China.

² Graduate School of Engineering Science, Osaka University, Japan.

³ Shenzhen Institute of Advanced Technology, Chinese Academy of Sciences, China.

⁴ Department of Electrical and Electronic Engineering, The Hong Kong Polytechnic University, Hong Kong SAR, China.

⁵ School of Transportation, Southeast University, China.

II. PRELIMINARIES

A. Markov Decision Processes

The interaction between the environment and RL agent is formulated as a Markov Decision Process (MDP) with a 5-tuple $(\mathcal{S}, \mathcal{A}, r, \mathcal{P}, \gamma)$, where \mathcal{S} and \mathcal{A} denote the state and action spaces, $r(\mathbf{s}, \mathbf{a})$ is the reward function, $\mathcal{P} : \mathcal{S} \times \mathcal{S} \times \mathcal{A} \mapsto [0, 1]$ is the transition probability, and $\gamma \in [0, 1]$ is the discount factor. The policy $\pi : \mathcal{S} \times \mathcal{A} \mapsto [0, 1]$ maps states to a distribution over actions. The objective is to find an optimal policy maximizing the value function:

$$V_\pi(\mathbf{s}) = \mathbb{E}_\pi \left[\sum_{t=0}^{\infty} \gamma^t r(\mathbf{s}_t, \mathbf{a}_t) \right]. \quad (1)$$

Let $\mathbf{s}' \sim \mathcal{P}(\mathbf{s}'|\mathbf{s}, \mathbf{a})$ and $\mathbf{a}' \sim \pi(\mathbf{a}'|\mathbf{s}')$. The corresponding state-action value function satisfies the Bellman equation:

$$Q_\pi(\mathbf{s}, \mathbf{a}) = r(\mathbf{s}, \mathbf{a}) + \gamma \mathbb{E}_{\mathbf{s}', \mathbf{a}'} [Q_\pi(\mathbf{s}', \mathbf{a}')]. \quad (2)$$

B. Actor-Critic Framework

The Actor-Critic (AC) framework integrates policy-based and value-based approaches through two components: the Actor $\pi(\mathbf{a}|\mathbf{s}; \phi)$, which represents the policy, and the Critic $Q(\mathbf{s}, \mathbf{a}; \theta)$, which estimates the action-value function. The Actor is updated by following the policy gradient using feedback from the Critic, while the Critic is trained to minimize the Temporal Difference (TD) error. This framework serves as the foundation for several advanced RL algorithms such as DDPG [37], SAC, and PPO, demonstrating its versatility in various control tasks.

III. APPROACH

A. Mix Entropy and Relative Entropy in Value Function

CSAC incorporates both entropy and relative entropy regularization into the value function. The augmented reward function is defined as:

$$r_{\text{CSAC}}(\mathbf{s}_t, \mathbf{a}_t) = r(\mathbf{s}_t, \mathbf{a}_t) + \gamma \sigma \mathbb{E}_{\mathbf{s}_{t+1}} [-\log(\pi(\cdot|\mathbf{s}_{t+1}))] - \gamma \tau \mathbb{E}_{\mathbf{s}_{t+1}} \left[\log \frac{\pi(\cdot|\mathbf{s}_{t+1})}{\tilde{\pi}(\cdot|\mathbf{s}_{t+1})} \right], \quad (3)$$

where σ and τ modulate the entropy and relative entropy terms, respectively. Substituting Eq. (3) into the Bellman equation (Eq. (2)) yields the CSAC value function:

$$Q_{\text{CSAC}}(\mathbf{s}_t, \mathbf{a}_t) = r(\mathbf{s}_t, \mathbf{a}_t) + \gamma \mathbb{E}_{\mathbf{s}_{t+1}, \mathbf{a}_{t+1}} [Q_{\text{CSAC}}(\mathbf{s}_{t+1}, \mathbf{a}_{t+1}) - \sigma \log(\pi(\mathbf{a}_{t+1}|\mathbf{s}_{t+1})) - \tau \log \frac{\pi(\mathbf{a}_{t+1}|\mathbf{s}_{t+1})}{\tilde{\pi}(\mathbf{a}_{t+1}|\mathbf{s}_{t+1})}] \quad (4)$$

Following TD3 [30] and SAC [19], we employ two critic networks $Q_{\text{CSAC}}^{\theta_1}$ and $Q_{\text{CSAC}}^{\theta_2}$ to mitigate overestimation. Given a sample $\{\mathbf{s}, \mathbf{a}, r(\mathbf{s}, \mathbf{a}), \mathbf{s}'\} \sim \mathcal{D}$ with $\mathbf{a}' \sim \pi(\cdot|\mathbf{s}')$, the critic loss is:

$$L(\theta_i) = \left[Q_{\text{CSAC}}^{\theta_i}(\mathbf{s}, \mathbf{a}) - y(\mathbf{s}, \mathbf{a}, \mathbf{s}') \right]^2, \quad i \in \{1, 2\} \quad (5)$$

where the TD target takes the minimum over two target networks (parameters $\hat{\theta}$):

$$y(\mathbf{s}, \mathbf{a}, \mathbf{s}') = r(\mathbf{s}, \mathbf{a}) + \gamma \left[\min_{j=1,2} Q_{\text{CSAC}}^{\hat{\theta}_j}(\mathbf{s}', \mathbf{a}') - \sigma \log(\pi(\mathbf{a}'|\mathbf{s}')) - \tau \log \frac{\pi(\mathbf{a}'|\mathbf{s}')}{\tilde{\pi}(\mathbf{a}'|\mathbf{s}')} \right] \quad (6)$$

Here the previous policy $\tilde{\pi}$ is iteratively stored and updated during learning to stabilize training.

B. Policy Improvement with Mixed Entropy and Relative Entropy Regularization

We now derive the actor update rule. Following SAC [19], the optimal policy for any state \mathbf{s} is:

$$\pi^* = \arg \max_{\pi} \sum_{\mathbf{a} \in \mathcal{A}} \pi(\mathbf{a}|\mathbf{s}) \left[Q_{\text{CSAC}}^*(\mathbf{s}, \mathbf{a}) - \sigma \log(\pi(\mathbf{a}|\mathbf{s})) - \tau \log \frac{\pi(\mathbf{a}|\mathbf{s})}{\tilde{\pi}(\mathbf{a}|\mathbf{s})} \right]. \quad (7)$$

For continuous action spaces, we solve Eq. (7) subject to $\int \pi(\mathbf{a}|\mathbf{s}) d\mathbf{a} = 1$ via the Lagrangian:

$$\mathcal{L}(\mathbf{s}, \lambda) = \int \pi(\mathbf{a}|\mathbf{s}) \left[Q_{\text{CSAC}}(\mathbf{s}, \mathbf{a}) + \sigma [-\log(\pi(\mathbf{a}|\mathbf{s}))] - \tau \left[\log \frac{\pi(\mathbf{a}|\mathbf{s})}{\tilde{\pi}(\mathbf{s}|\mathbf{s})} \right] \right] d\mathbf{a} - \lambda \left(\int \pi(\mathbf{a}|\mathbf{s}) d\mathbf{a} - 1 \right). \quad (8)$$

Setting $\partial \mathcal{L} / \partial \pi = 0$ and following CVI [32] with $\alpha = \frac{\tau}{\tau + \sigma}$ and $\beta = \frac{1}{\tau + \sigma}$, we obtain:

$$\pi(\mathbf{a}|\mathbf{s}) = \tilde{\pi}^\alpha(\mathbf{a}|\mathbf{s}) e^{(-\beta\lambda - 1)} e^{\beta Q_{\text{CSAC}}(\mathbf{s}, \mathbf{a})}. \quad (9)$$

Applying the normalization condition to solve for λ and combining with Eq. (9), the updated policy at iteration k is:

$$\pi_{k+1}(\mathbf{a}|\mathbf{s}) = \frac{\pi_k^\alpha(\mathbf{a}|\mathbf{s}) \exp(\beta Q_{\text{CSAC}, k+1}(\mathbf{s}, \mathbf{a}))}{\int \pi_k^\alpha(\mathbf{a}|\mathbf{s}) \exp(\beta Q_{\text{CSAC}, k+1}(\mathbf{s}, \mathbf{a})) d\mathbf{a}}. \quad (10)$$

Introducing the action preference function P [1], [31], this can be expressed as:

$$P_{k+1}(\mathbf{s}, \mathbf{a}) = \frac{\alpha}{\beta} \log \pi_k(\mathbf{a}|\mathbf{s}) + Q_{\text{CSAC}, k+1}(\mathbf{s}, \mathbf{a}), \quad (11)$$

$$V_{\text{CSAC}, k}(\mathbf{s}) = \frac{1}{\beta} \log \int \exp(\beta P_k(\mathbf{s}, \mathbf{a})) d\mathbf{a}, \quad (12)$$

$$\pi_k(\mathbf{a}|\mathbf{s}) = \exp(\beta (P_k(\mathbf{s}, \mathbf{a}) - V_{\text{CSAC}, k}(\mathbf{s}))). \quad (13)$$

Eq. (10) conforms to the Energy-Based Policy (EBP) model [19], which cannot be sampled directly. Following [19], [38], we approximate it with a Gaussian policy by minimizing the KL divergence. For $\mathbf{s} \sim \mathcal{D}$, the actor loss is:

$$J_\pi(\phi) = D_{\text{KL}}[\pi(\cdot|\mathbf{s}) \parallel \exp \beta (P(\mathbf{s}, \cdot) - V_{\text{CSAC}}(\mathbf{s}))] = \mathbb{E}_{\mathbf{a} \sim \pi} [\log \pi(\mathbf{a}|\mathbf{s}) - \beta P(\mathbf{s}, \mathbf{a}) + \beta V_{\text{CSAC}}(\mathbf{s})]. \quad (14)$$

The actor generates actions via the reparameterization trick:

$$\tilde{\mathbf{a}}(\mathbf{s}, \boldsymbol{\xi}) = \tanh(\mu(\mathbf{s}) + \sigma(\mathbf{s}) \odot \boldsymbol{\xi}), \quad \boldsymbol{\xi} \sim \mathcal{N}(\mathbf{0}, \mathbf{I}), \quad (15)$$

Algorithm 1: Conservative Soft Actor-Critic

Initialize memory buffer \mathcal{D} , soft update rate ρ , σ and τ that control entropy and relative entropy terms, critic networks $Q^{\theta_1}, Q^{\theta_2}$, target critic networks $Q^{\hat{\theta}_1}, Q^{\hat{\theta}_2}$ with copied parameters $\hat{\theta}_1 \leftarrow \theta_1, \hat{\theta}_2 \leftarrow \theta_2$, actor network π_ϕ and previous actor networks π^{ϕ_p} with current weights: $\phi_p \leftarrow \phi$

for $t = 1$ to T_{initial} **do**

- # Collect sample with a random policy
- $\mathcal{D} \leftarrow (s_t, \mathbf{a}_t, r(s_t, \mathbf{a}_t), s_{t+1})$

for $t = 1$ to T **do**

- # Interaction phase
- Observe state s_t
- Decide and execute action $\mathbf{a}_t \sim \pi^\phi(\mathbf{a}_t | s_t)$
- Observe next state s_{t+1} and get reward $r(s_t, \mathbf{a}_t)$
- $\mathcal{D} \leftarrow (s_t, \mathbf{a}_t, r(s_t, \mathbf{a}_t), s_{t+1})$
- # Update phase
- $\phi_p \leftarrow \phi$
- Random sample mini-batch of M tuples from \mathcal{D}
- for** each sampled tuple $(s, \mathbf{a}, r(s, \mathbf{a}), s')$ **do**

 - # Calculate TD error following Eq. (6)
 - $\mathbf{a}' \sim \pi^\phi(\cdot | s')$
 - $y(s, \mathbf{a}, s') = r(s, \mathbf{a}) + \gamma(\min_{j=1,2} Q^{\hat{\theta}_j}(s', \mathbf{a}') - \sigma \log(\pi^\phi(\mathbf{a}' | s')) - \tau \log \frac{\pi^\phi(\mathbf{a}' | s')}{\pi_{\phi_p}(\mathbf{a}' | s')})$
 - # Update critic networks following Eq. (5)
 - $\nabla_{\theta_i} [Q^{\theta_i}(s, \mathbf{a}) - y(s, \mathbf{a}, s')]^2$, for $i \in \{1, 2\}$
 - # Update actor networks following Eq. (16)
 - $\nabla_{\phi} (\tau + \sigma) \log \pi^\phi(\tilde{\mathbf{a}}(s, \xi) | s) - \tau \log \pi^{\phi_p}(\tilde{\mathbf{a}}(s, \xi)_t | s) - \min_{i=1,2} (Q^{\theta_i}(s, \tilde{\mathbf{a}}(s, \xi)))$
 - # Update target networks weights
 - $\hat{\theta}_i \leftarrow \rho \theta_i + (1 - \rho) \hat{\theta}_i$ for $i \in \{1, 2\}$

return $Q^{\theta_1}(\cdot), Q^{\theta_2}(\cdot), \pi^\phi(\cdot)$

where $\mu(s)$ and $\sigma(s)$ are the mean and variance. Dividing Eq. (14) by β and omitting the intractable normalization term, the practical actor loss becomes:

$$J_\pi(\phi) \approx (\tau + \sigma) \log \pi(\tilde{\mathbf{a}}(s, \xi) | s) - \tau \log \tilde{\pi}(\tilde{\mathbf{a}}(s, \xi) | s) - \min_{i=1,2} (Q_{\text{CSAC}}^{\theta_i}(s, \tilde{\mathbf{a}}(s, \xi))), \quad (16)$$

where the action preference function uses the minimum critic output:

$$P(s, \tilde{\mathbf{a}}(s, \xi)) = \tau \log \tilde{\pi}(\tilde{\mathbf{a}}(s, \xi) | s) + \min_{i=1,2} (Q_{\text{CSAC}}^{\theta_i}(s, \tilde{\mathbf{a}}(s, \xi))). \quad (17)$$

C. Summary of Conservative Soft Actor-Critic

The complete CSAC algorithm is summarized in Algorithm 1. After initializing the networks and collecting initial samples with a random policy, CSAC alternates between an interaction phase (collecting experience into replay buffer

\mathcal{D}) and an update phase. In each update, the previous actor parameters are stored, and a mini-batch is sampled from \mathcal{D} to update the critic (Eq. (5)) and actor (Eq. (16)) networks via gradient descent, followed by soft updates of the target networks controlled by ρ .

IV. EXPERIMENTS

A. Experimental Settings

We evaluated CSAC on four MuJoCo benchmark tasks [39], [40], including HalfCheetah-v4, Walker2d-v4, Ant-v4, and Hopper-v4, which cover diverse robotic structures and dynamic control challenges. The task specifications are shown in Fig. 1 and Table II.

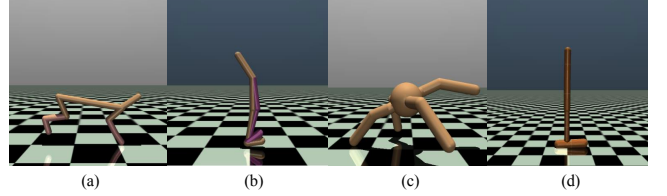


Fig. 1: Benchmark tasks for evaluation in this article. (a) HalfCheetah-v4. (b) Walker2d-v4. (c) Ant-v4. (d) Hopper-v4.

TABLE II: Observation and Action Spaces for Different MuJoCo Tasks

	Observation Space	Action Space
HalfCheetah-v4	17	6
Walker2d-v4	17	6
Ant-v4	27	8
Hopper-v4	11	3

We compared CSAC against four baselines: SAC [19], PPO [25], TD3 [30], and the recent SD3 [41], spanning both on-policy and off-policy approaches. All results are averaged over five independent trials. CSAC was implemented using PaddlePaddle [42] with its RL toolkit PARL, and experiments were conducted on a server with an Intel Xeon Gold-6248R CPU, NVIDIA RTX-A5000 GPU, and 256 GB RAM (Ubuntu 20.04).

Common hyperparameters are listed in Table III. For CSAC, the entropy coefficient σ was set to 0.2 and the relative entropy coefficient τ to 0.5 across all MuJoCo tasks.

B. Evaluation of Learning Capability on MuJoCo Tasks

The learning curves and maximum average returns are shown in Fig. 2 and Table IV (best results in red). CSAC achieved the highest returns in HalfCheetah-v4, Walker2d-v4, and Ant-v4, outperforming SAC by 5.6%, 51.5%, and 5.9%, respectively, and surpassing PPO, TD3, and SD3 by wider margins. In Walker2d-v4, where balancing and gait control are particularly challenging, CSAC's relative entropy regularization effectively prevented excessive policy updates, yielding the largest improvement over baselines. In Hopper-v4, CSAC performed comparably to SD3 (3458.22

TABLE III: COMMON HYPER-PARAMETER SETTINGS OF COMPARED APPROACHES

	CSAC(ours)	SAC	PPO	TD3	SD3
Critic Learning Rate	$3 \cdot 10^{-4}$	$3 \cdot 10^{-4}$	$3 \cdot 10^{-4}$	$3 \cdot 10^{-4}$	$1 \cdot 10^{-3}$
Actor Learning Rate	$3 \cdot 10^{-4}$	$3 \cdot 10^{-4}$	$3 \cdot 10^{-4}$	$3 \cdot 10^{-4}$	$1 \cdot 10^{-3}$
Actor and Critic Structure	(256,256)	(256,256)	(64,64)	(256,256)	(256,256)
Target Update Rate	0.005	0.005	/	0.005	0.005
Batch Size	256	256	32	256	256
Memory Size	$1 \cdot 10^6$	$1 \cdot 10^6$	/	$1 \cdot 10^6$	$1 \cdot 10^6$
Warmup Steps	$1 \cdot 10^4$	$1 \cdot 10^4$	/	$1 \cdot 10^4$	$1 \cdot 10^4$
Discount Factor	0.99	0.99	0.99	0.99	0.99

vs. 3515.30) while still substantially outperforming SAC (+13.9%) and PPO (+56.9%). Overall, the joint entropy and relative entropy regularization enables CSAC to balance exploration and exploitation effectively, leading to superior and stable convergence across diverse continuous control tasks.

C. Ablation Study on Walker2d Task

Since the effect of the entropy coefficient has been extensively studied in SAC-related literature [19], [43], we focus on the relative entropy coefficient τ . Fig. 3 shows CSAC’s learning curves in Walker2d-v4 under τ values ranging from 0.005 to 50.0.

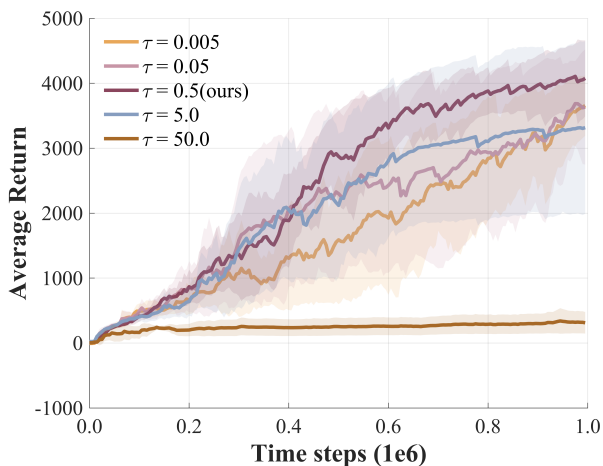


Fig. 3: Learning curves of CSAC with different τ values in the Walker2d-v4 task. The shaded region represents the standard deviation of the average evaluation over five trials. Curves are smoothed uniformly for visual clarity.

The results reveal a clear sensitivity to τ . Small values ($\tau = 0.005, 0.05$) weaken the reverse KL divergence constraint, causing the policy to focus on high-probability regions and reducing exploration, which leads to suboptimal convergence. The default setting $\tau = 0.5$ achieves the best performance, with final returns approaching 4000, effectively balancing exploration and exploitation. Conversely, large values ($\tau = 5.0, 50.0$) over-constrain policy updates, making the policy overly conservative and resulting in stagnating returns. These results confirm that a moderate τ is critical for optimal performance.

D. Evaluation of Sample Efficiency

We define sample efficiency as the number of interactions required to reach the lower boundary of the maximum average returns in Table IV—a metric critical for real-world deployment where sampling costs are high. Results are presented in Fig. 4 and Table V (best results in red).

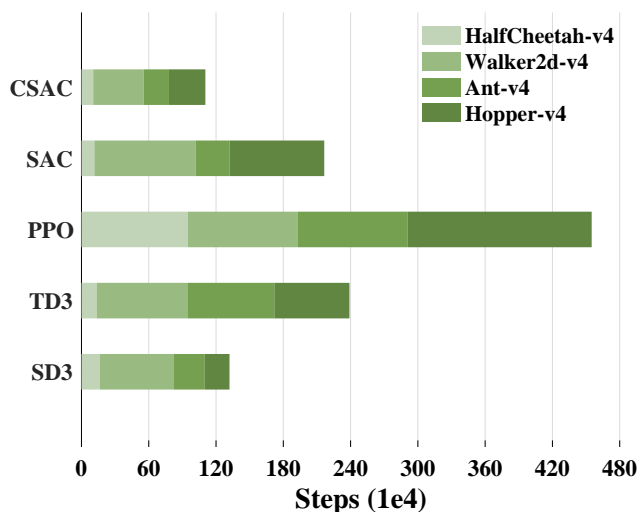


Fig. 4: Number of interactions used by all compared approaches to reach the lower boundary of the maximum average returns over four benchmark control tasks.

TABLE V: Number of Interactions Required to Reach the Lower Bound of Maximum Average Return (in 10^4 Steps)

	HalfCheetah-v4	Walker2d-v4	Ant-v4	Hopper-v4
CSAC	10.5	45	22.5	32.5
SAC	11.5	90.5	30	84.5
PPO	95	98	98	164
TD3	13.5	81.5	77	67
SD3	16.5	65.5	28	22

CSAC achieved the fewest interaction steps in three of four tasks. In HalfCheetah-v4, it required only 105,000 steps, reducing the count by 8.7% vs. SAC and over 8-fold vs. PPO. In Walker2d-v4 and Ant-v4, CSAC improved sample efficiency over SAC by 50.3% and 25%, respectively, and outperformed all other baselines by even wider margins. In Hopper-v4, SD3 was slightly more efficient (220,000 vs. 325,000 steps), yet CSAC still reduced steps by

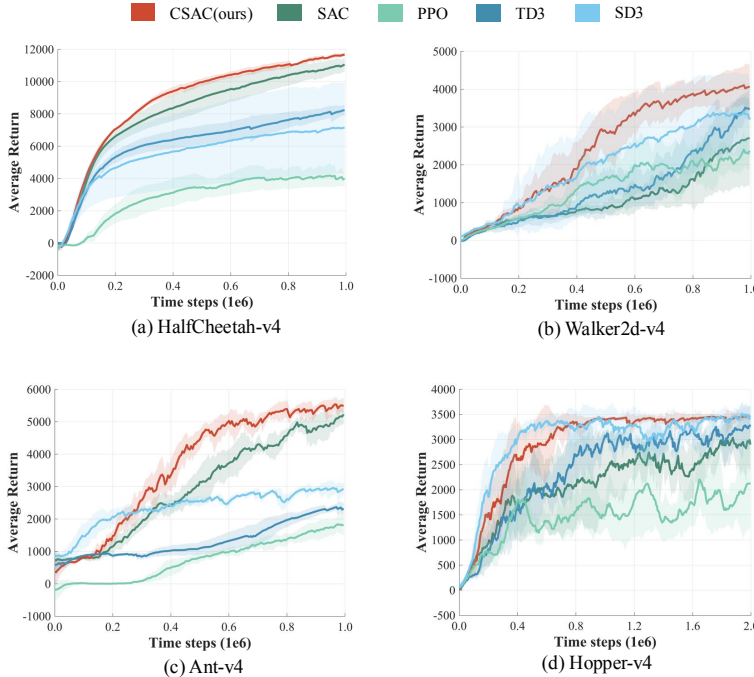


Fig. 2: Learning curves over four benchmark tasks. Curves are uniformly smoothed for visual clarity. The shaded region represents the corresponding standard deviation.

TABLE IV: Maximum average returns over four benchmark tasks

	CSAC (ours)	SAC	PPO	TD3	SD3
HalfCheetah-v4	11672.74 ± 151.21	11052.89 ± 422.84	4181.89 ± 723.54	8224.70 ± 337.13	7158.19 ± 2821.74
Walker2d-v4	4106.21 ± 501.45	2710.65 ± 1272.01	2403.55 ± 502.86	3513.25 ± 295.81	3404.03 ± 989.50
Ant-v4	5538.20 ± 209.62	5229.39 ± 269.52	1836.47 ± 233.91	2368.35 ± 99.15	2960.61 ± 212.54
Hopper-v4	3458.22 ± 59.87	3037.19 ± 242.06	2204.01 ± 540.71	3296.80 ± 356.86	3515.30 ± 107.84

61.5% compared to SAC. These results confirm that the joint entropy and relative entropy regularization enables CSAC to converge rapidly with fewer environment interactions across diverse tasks.

E. Evaluation of Robustness in HalfCheetah Task

To assess robustness under dynamic perturbations, we compared CSAC with SAC—chosen for its structural similarity—in HalfCheetah-v4, where friction was suddenly increased to $1.5\times$, $2.0\times$, and $2.5\times$ its original value after 300,000 steps of standard training. The results are shown in Fig. 5.

At $1.5\times$ friction (left panel), both algorithms experienced return fluctuations, but CSAC recovered faster and maintained higher evaluation returns. As friction rose to $2.0\times$ (middle panel), SAC’s performance became increasingly erratic, whereas CSAC recovered more quickly and consistently sustained a higher return level during evaluation. At the most challenging $2.5\times$ friction (right panel), CSAC again exhibited a smaller performance decline and faster adaptation, while SAC showed severe instability and failed to recover to its initial level. Across all noise intensities, CSAC consistently demonstrated faster recovery and greater stability than SAC, confirming the effectiveness of relative

TABLE VI: Observation and Action Spaces for Two Real-Robot-Based Simulation Tasks

	Observation Space	Action Space
QuadX-Waypoints-v1	9	4
PandaReach-v2	17	6

entropy regularization in enhancing robustness under dynamic perturbations.

F. Implementation on Real-Robot-Based Simulation

1) *Experimental Settings for Real-Robot-Based Simulation Experiments:* We employed two PyBullet-based simulation platforms [44]—PyFlyt [45] and Panda Gym [46]—to evaluate CSAC in real-robot-based simulations (Fig. 6, Table VI). The QuadX-Waypoints-v1 task (Fig. 6a) requires a quadrotor UAV to navigate through four designated waypoints, while the PandaReach-v2 task (Fig. 6b) requires a Panda robotic arm to move its end-effector to a target position.

Common parameters follow Table III; CSAC-specific hyperparameters (σ , τ) are listed in Table VII. All experiments were averaged over five independent trials.

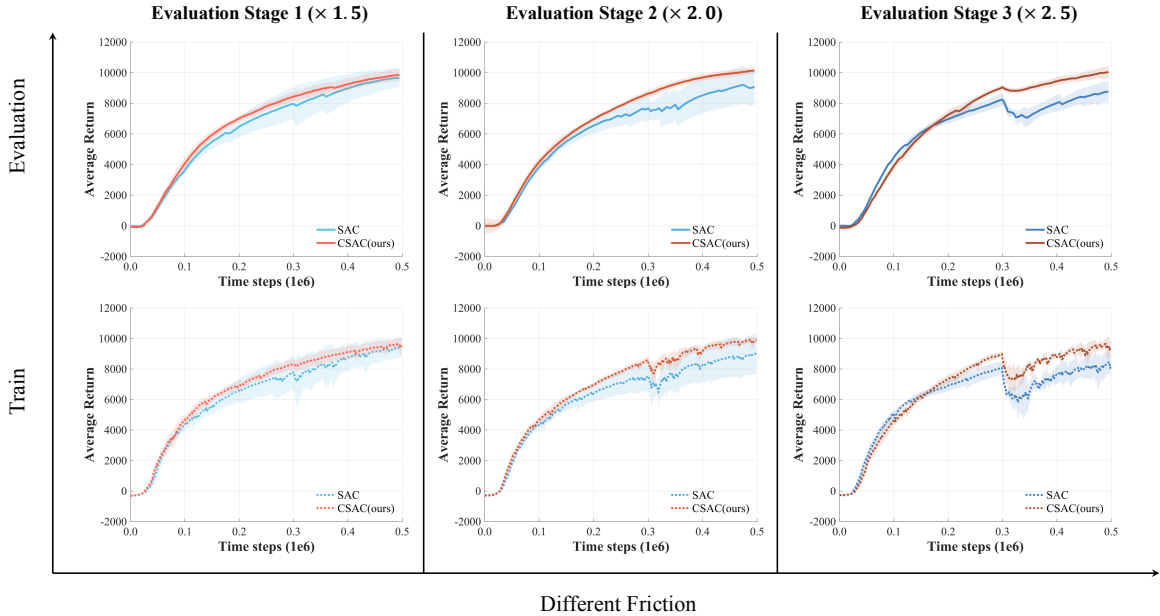


Fig. 5: Performance comparison of CSAC and SAC under varying Friction-Induced dynamic noise in the HalfCheetah-v4 environment. The shaded region represents the corresponding standard deviation.

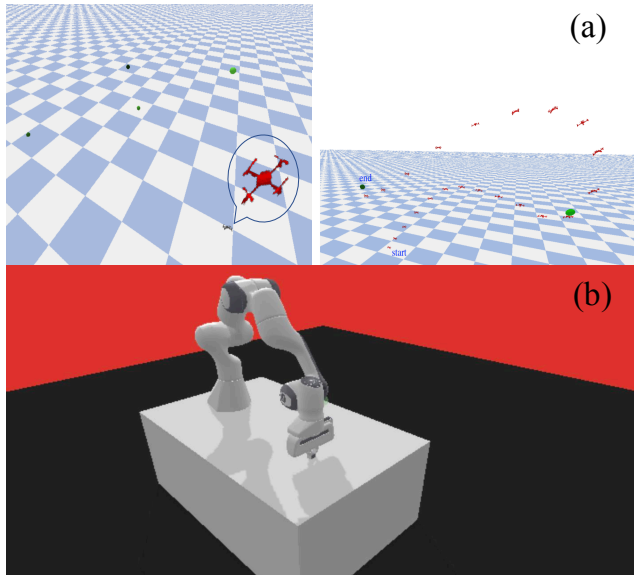


Fig. 6: Real-Robot-Based simulation experiments for evaluation in this article. (a) QuadX-Waypoints-v1. (b) PandaReach-v2.

TABLE VII: SPECIFIC HYPERPARAMETERS OF CSAC

	σ	τ
QuadX-Waypoints-v1	0.2	0.1
PandaReach-v2	0.2	0.5

2) *Evaluation of the Learning Capability on Two Real-Robot-Based Simulation Tasks:* The learning curves and maximum average returns are shown in Fig. 7 and Table VIII (best results in red).

In QuadX-Waypoints-v1, CSAC achieved a final average return of 530.28, outperforming SAC by 36.5%, TD3 by 22.3%, PPO by 98.6%, and SD3 by 38.5%. In PandaReach-v2, which demands high-precision control, CSAC (-2.04) slightly improved upon SAC (-2.12) while exhibiting lower variance; PPO, TD3, and SD3 all performed poorly (returns < -48), highlighting their deficiency in fine control tasks. Overall, CSAC demonstrated superior and stable performance across both real-robot-based tasks.

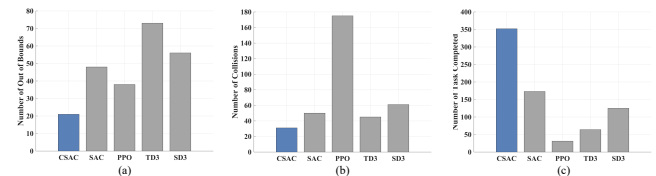


Fig. 8: The average number of each condition in QuadX-Waypoints-v1: (a) Number of out of bounds; (b) Number of collisions; (c) Number of task completed.

TABLE IX: Case Analysis in QuadX-Waypoints-v1

	Out of Bound	Collision	Completion
CSAC	20.6 ± 11.24	31.6 ± 10.41	352.0 ± 241.57
SAC	48.2 ± 27.54	50.6 ± 14.36	173.4 ± 230.56
PPO	38.4 ± 17.93	175.4 ± 4.16	31.0 ± 19.67
TD3	73.2 ± 20.5	45.4 ± 15.01	64.0 ± 68.31
SD3	56.0 ± 18.72	61.2 ± 24.34	125.4 ± 158.86

3) *Evaluation of Robustness in Drones Control:* We evaluated the robustness of learned policies in QuadX-Waypoints-v1 by recording out-of-bounds, collision, and successful completion counts over 1000 evaluation rollouts

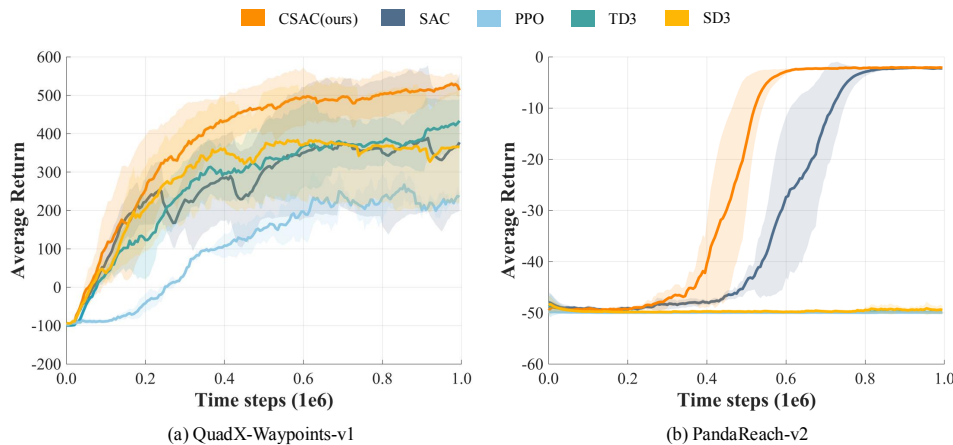


Fig. 7: Learning curves of two Real-Robot-Based simulation tasks. The shaded region represents the standard deviation of the average evaluation over five independent trials. Curves are uniformly smoothed for visual clarity.

TABLE VIII: MAX AVERAGE RETURNS OVER two Real-Robot-Based simulation TASKS

	CSAC (ours)	SAC	PPO	TD3	SD3
QuadX-Waypoints-v1	530.28 ± 29.04	388.55 ± 189.51	267.06 ± 32.07	433.56 ± 56.03	383.03 ± 145.51
PandaReach-v2	-2.04 ± 0.18	-2.12 ± 0.22	-49.80 ± 0.04	-48.57 ± 0.08	-48.36 ± 0.10

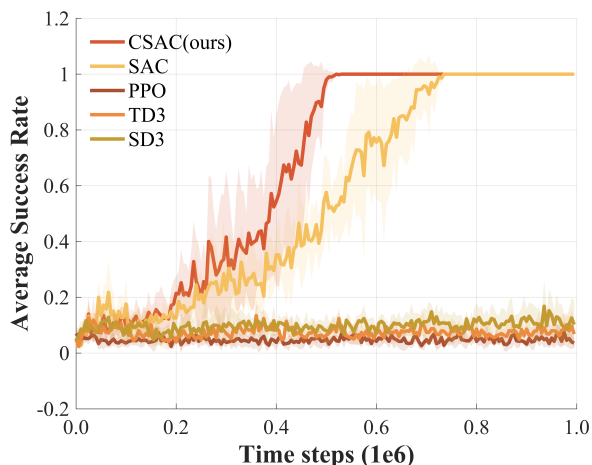


Fig. 9: The average success rate in PandaReach-v2.

per trial (five trials total). Results are shown in Fig. 8 and Table IX (best results in red). CSAC achieved the fewest failures and the most completions among all methods, reducing out-of-bounds by 46.3% vs. PPO and collisions by 30.4% vs. TD3, while completing over 350 rollouts successfully—close to the sum of all four baselines combined. These results confirm that the joint regularization enables effective exploration while preventing the overly aggressive policy updates that lead to unstable drone control.

4) *Evaluation of Effectiveness in Robotic Arm:* We further evaluated the average success rate in PandaReach-v2 (Fig. 9). CSAC’s success rate rose rapidly around 400,000 steps and reached nearly 100% by 600,000 steps, whereas SAC converged noticeably slower (around 800,000 steps)

with a slightly lower final rate. PPO, TD3, and SD3 exhibited large fluctuations and failed to achieve effective policy learning, indicating their inability to meet the high-precision demands of this task. These results confirm CSAC’s effectiveness and fast convergence in fine control scenarios.

V. CONCLUSION

This paper introduces Conservative Soft Actor-Critic (CSAC), which integrates entropy and relative entropy regularization into the Actor-Critic framework to enhance both exploration and stability for robot control. Experiments on four MuJoCo benchmark tasks and two real-robot-based simulation tasks demonstrate that CSAC achieves superior learning capability, sample efficiency, and robustness over state-of-the-art baselines, confirming the benefit of jointly leveraging both regularization terms.

For future work, we plan to develop adaptive strategies for dynamically adjusting σ and τ to optimize the exploration-exploitation trade-off, and to deploy CSAC on real-world hardware such as UAVs and robotic arms to validate its effectiveness under physical constraints and real-time decision-making requirements.

REFERENCES

- [1] R. S. Sutton and A. G. Barto, *Reinforcement learning: An introduction*. MIT press, 2018.
- [2] J. Kober, J. A. Bagnell, and J. Peters, “Reinforcement learning in robotics: A survey,” *The International Journal of Robotics Research*, vol. 32, no. 11, pp. 1238–1274, 2013.
- [3] V. Mnih, K. Kavukcuoglu, D. Silver, A. A. Rusu, J. Veness, M. G. Bellemare, A. Graves, M. Riedmiller, A. K. Fidjeland, G. Ostrovski *et al.*, “Human-level control through deep reinforcement learning,” *Nature*, vol. 518, no. 7540, pp. 529–533, 2015.
- [4] D. Silver, T. Hubert, J. Schrittwieser, I. Antonoglou, M. Lai, A. Guez, M. Lanctot, L. Sifre, D. Kumaran, T. Graepel *et al.*, “A general reinforcement learning algorithm that masters chess, shogi, and go through self-play,” *Science*, vol. 362, no. 6419, pp. 1140–1144, 2018.

- [5] E. Kaufmann, L. Bauersfeld, A. Loquercio, M. Müller, V. Koltun, and D. Scaramuzza, "Champion-level drone racing using deep reinforcement learning," *Nature*, vol. 620, no. 7976, pp. 982–987, 2023.
- [6] Z. Wang, Y. Jia, L. Shi, H. Wang, H. Zhao, X. Li, J. Zhou, J. Ma, and G. Zhou, "Arm-constrained curriculum learning for loco-manipulation of the wheel-legged robot," *arXiv preprint arXiv:2403.16535*, 2024.
- [7] C. Miao, Y. Cui, H. Li, and X. Wu, "Effective multi-agent deep reinforcement learning control with relative entropy regularization," *IEEE Transactions on Automation Science and Engineering*, 2024.
- [8] I. Goodfellow, Y. Bengio, and A. Courville, *Deep learning*. MIT Press, 2016.
- [9] T. P. Lillicrap, J. J. Hunt, A. Pritzel, N. Heess, T. Erez, Y. Tassa, D. Silver, and D. Wierstra, "Continuous control with deep reinforcement learning," in *International Conference on Learning Representations (ICLR)*, 2016.
- [10] L. Zhu, Y. Cui, and T. Matsubara, "Dynamic actor-advisor programming for scalable safe reinforcement learning," in *2020 IEEE International Conference on Robotics and Automation (ICRA)*. IEEE, 2020, pp. 10 681–10 687.
- [11] Y. Cui, S. Osaki, and T. Matsubara, "Autonomous boat driving system using sample-efficient model predictive control-based reinforcement learning approach," *Journal of Field Robotics*, vol. 38, no. 3, pp. 331–354, 2021.
- [12] D. Chen, H. Li, Z. Jin, and H. Tu, "Risk-anticipatory autonomous driving strategies considering vehicles' weights, based on hierarchical deep reinforcement learning," *arXiv preprint arXiv:2401.08661*, 2023.
- [13] R. Yan, R. Jiang, B. Jia, J. Huang, and D. Yang, "Hybrid car-following strategy based on deep deterministic policy gradient and cooperative adaptive cruise control," *IEEE Transactions on Automation Science and Engineering*, vol. 19, no. 4, pp. 2816–2824, 2021.
- [14] B. Cai, C. Wei, and Z. Ji, "Deep reinforcement learning with multiple unrelated rewards for agv mapless navigation," *IEEE Transactions on Automation Science and Engineering*, 2024.
- [15] Y. Zhou, Y. Jin, P. Lu, S. Jiang, Z. Wang, and B. He, "T-td3: A reinforcement learning framework for stable grasping of deformable objects using tactile prior," *IEEE Transactions on Automation Science and Engineering*, 2024.
- [16] H. Zhu, J. Yu, A. Gupta, D. Shah, K. Hartikainen, A. Singh, V. Kumar, and S. Levine, "The ingredients of real world robotic reinforcement learning," in *International Conference on Learning Representations*, 2020. [Online]. Available: <https://openreview.net/forum?id=rJe2syrtvS>
- [17] G. Dulac-Arnold, N. Levine, D. J. Mankowitz, J. Li, C. Paduraru, S. Gowal, and T. Hester, "Challenges of real-world reinforcement learning: definitions, benchmarks and analysis," *Machine Learning*, vol. 110, no. 9, pp. 2419–2468, 2021.
- [18] O. Kroemer, S. Niekum, and G. Konidaris, "A review of robot learning for manipulation: Challenges, representations, and algorithms," *Journal of machine learning research*, vol. 22, no. 30, pp. 1–82, 2021.
- [19] T. Haarnoja, A. Zhou, P. Abbeel, and S. Levine, "Soft actor-critic: Off-policy maximum entropy deep reinforcement learning with a stochastic actor," in *International conference on machine learning*. PMLR, 2018, pp. 1861–1870.
- [20] R. Ma, Y. Wang, S. Wang, L. Cheng, R. Wang, and M. Tan, "Sample-observed soft actor-critic learning for path following of a biomimetic underwater vehicle," *IEEE Transactions on Automation Science and Engineering*, pp. 1–10, 2023.
- [21] A. Wahid, A. Stone, K. Chen, B. Ichter, and A. Toshev, "Learning object-conditioned exploration using distributed soft actor critic," in *Conference on Robot Learning*. PMLR, 2021, pp. 1684–1695.
- [22] Z. He, L. Dong, C. Song, and C. Sun, "Multiagent soft actor-critic based hybrid motion planner for mobile robots," *IEEE transactions on neural networks and learning systems*, 2022.
- [23] K. Nakhleh, M. Raza, M. Tang, M. Andrews, R. Boney, I. Hadžić, J. Lee, A. Mohajeri, and K. Palyutina, "Sacplanner: Real-world collision avoidance with a soft actor critic local planner and polar state representations," in *2023 IEEE International Conference on Robotics and Automation (ICRA)*. IEEE, 2023, pp. 9464–9470.
- [24] J. Schulman, S. Levine, P. Abbeel, M. Jordan, and P. Moritz, "Trust region policy optimization," in *International conference on machine learning*. PMLR, 2015, pp. 1889–1897.
- [25] J. Schulman, F. Wolski, P. Dhariwal, A. Radford, and O. Klimov, "Proximal policy optimization algorithms," *arXiv preprint arXiv:1707.06347*, 2017.
- [26] D. Xue, D. Wu, A. S. Yamashita, and Z. Li, "Proximal policy optimization with reciprocal velocity obstacle based collision avoidance path planning for multi-unmanned surface vehicles," *Ocean Engineering*, vol. 273, p. 114005, 2023.
- [27] P. Sadhukhan and R. R. Selmic, "Multi-agent formation control with obstacle avoidance using proximal policy optimization," in *2021 IEEE International Conference on Systems, Man, and Cybernetics (SMC)*. IEEE, 2021, pp. 2694–2699.
- [28] Y. Guan, Y. Ren, S. E. Li, Q. Sun, L. Luo, and K. Li, "Centralized cooperation for connected and automated vehicles at intersections by proximal policy optimization," *IEEE Transactions on Vehicular Technology*, vol. 69, no. 11, pp. 12 597–12 608, 2020.
- [29] E. Bøhn, E. M. Coates, S. Moe, and T. A. Johansen, "Deep reinforcement learning attitude control of fixed-wing uavs using proximal policy optimization," in *2019 international conference on unmanned aircraft systems (ICUAS)*. IEEE, 2019, pp. 523–533.
- [30] S. Fujimoto, H. Hoof, and D. Meger, "Addressing function approximation error in actor-critic methods," in *International Conference on Machine Learning (ICML)*, 2018.
- [31] M. G. Azar, V. Gómez, and H. J. Kappen, "Dynamic policy programming," *The Journal of Machine Learning Research*, vol. 13, no. 1, pp. 3207–3245, 2012.
- [32] T. Kozuno, E. Uchibe, and K. Doya, "Theoretical analysis of efficiency and robustness of softmax and gap-increasing operators in reinforcement learning," in *International Conference on Artificial Intelligence and Statistics (AISTATS)*, 2019.
- [33] Y. Cui, T. Matsubara, and K. Sugimoto, "Kernel dynamic policy programming: Applicable reinforcement learning to robot systems with high dimensional states," *Neural Networks*, vol. 94, pp. 13–23, 2017.
- [34] Y. Tsurumine, Y. Cui, E. Uchibe, and T. Matsubara, "Deep reinforcement learning with smooth policy update: Application to robotic cloth manipulation," *Robotics and Autonomous Systems*, vol. 112, pp. 72–83, 2019.
- [35] Z. Shang, H. Li, and Y. Cui, "Shiftable dynamic policy programming for efficient and robust reinforcement learning control," in *2021 IEEE International Conference on Robotics and Biomimetics (ROBIO)*. IEEE, 2021, pp. 1688–1693.
- [36] Z. Shang, R. Li, C. Zheng, H. Li, and Y. Cui, "Relative entropy regularized sample-efficient reinforcement learning with continuous actions," *IEEE Transactions on Neural Networks and Learning Systems*, 2023.
- [37] T. P. Lillicrap, J. J. Hunt, A. Pritzel, N. Heess, T. Erez, Y. Tassa, D. Silver, and D. Wierstra, "Continuous control with deep reinforcement learning," *arXiv preprint arXiv:1509.02971*, 2015.
- [38] T. Haarnoja, H. Tang, P. Abbeel, and S. Levine, "Reinforcement learning with deep energy-based policies," in *International conference on machine learning*. PMLR, 2017, pp. 1352–1361.
- [39] E. Todorov, T. Erez, and Y. Tassa, "Mujoco: A physics engine for model-based control," in *2012 IEEE/RSJ international conference on intelligent robots and systems*. IEEE, 2012, pp. 5026–5033.
- [40] M. Towers, A. Kwiatkowski, J. Terry, J. U. Balis, G. De Cola, T. Deleu, M. Goulão, A. Kallinteris, M. Krimmel, A. KG *et al.*, "Gymnasium: A standard interface for reinforcement learning environments," *arXiv preprint arXiv:2407.17032*, 2024.
- [41] L. Pan, Q. Cai, and L. Huang, "Softmax deep double deterministic policy gradients," *Advances in Neural Information Processing Systems*, vol. 33, pp. 11 767–11 777, 2020.
- [42] Y. Ma, D. Yu, T. Wu, and H. Wang, "PaddlePaddle: An open-source deep learning platform from industrial practice," *Frontiers of Data and Computing*, vol. 1, no. 1, pp. 105–115, 2019.
- [43] T. Haarnoja, A. Zhou, K. Hartikainen, G. Tucker, S. Ha, J. Tan, V. Kumar, H. Zhu, A. Gupta, P. Abbeel *et al.*, "Soft actor-critic algorithms and applications," *arXiv preprint arXiv:1812.05905*, 2018.
- [44] E. Coumans and Y. Bai, "Pybullet, a python module for physics simulation for games, robotics and machine learning," <http://pybullet.org>, 2016–2021.
- [45] J. J. Tai, J. Wong, M. Innocente, N. Horri, J. Brusey, and S. K. Phang, "Pyflyt-uav simulation environments for reinforcement learning research," *arXiv preprint arXiv:2304.01305*, 2023.
- [46] Q. Gallowédec, N. Cazin, E. Dellandréa, and L. Chen, "panda-gym: Open-Source Goal-Conditioned Environments for Robotic Learning," *4th Robot Learning Workshop: Self-Supervised and Lifelong Learning at NeurIPS*, 2021.